Transfer Learning in Keratoconus Classification

https://doi.org/10.3991/ijoe.v18i15.33689

Mustapha Aatila[1(✉)], Mohamed Lachgar[1], Hamid Hrimech[2], Ali Kartit[1]
[1]LTI, National School of Applied Sciences of El Jadida, El Jadida, Morocco
[2]LAMSAD, National School of Applied Sciences of Berrechid, Berrechid, Morocco
aatila.m@ucd.ac.ma

Abstract—Early detection of keratoconus will provide more treatment choices, avoid heavy treatments, and help stop the rapid progression of the disease. This study presents a machine learning-based keratoconus classification approach, using transfer learning, applied on corneal topographic images. Classification is performed considering the three corneal classes namely: normal, suspicious and keratoconus. Keratoconus classification is carried out using transfer learning, by the adoption of six different pretrained convolutional neural networks (CNN) VGG16, InceptionV3, MobileNet, DenseNet201, Xception and EfficientNetB0, which already have knowledge from solving previous specific problems. Each of these different classifiers is trained individually on five different datasets, generated from an original dataset of 2924 corneal topographic images. Original corneal topographic images have been subjected to a special preprocessing before their use by different models in the learning phase. Images of corneal maps are separated in five different datasets while removing noise and textual annotation from images. Most of models used in the classification allow good discrimination between normal cornea, suspicious and keratoconus one. Obtained results reached classification accuracy of 99.31% and 98.51% by DenseNet201 and VGG16 respectively. Obtained results indicate that transfer learning technique could well improve performance of keratoconus classification systems.

Keywords—keratoconus classification, machine learning, deep learning, transfer learning, corneal topography

1 Introduction

Keratoconus is a progressive disorder of the cornea, which gradually thins to take the form of an irregular cone [1]. Keratoconus is often causing myopia, irregular astigmatism, a decrease in visual acuity and an appearance of corneal opacities at an advanced stage [2]. It usually affects both eyes, but not with the same severity [3]. Figure 1 below indicates the difference between a normal cornea and a keratoconus one.

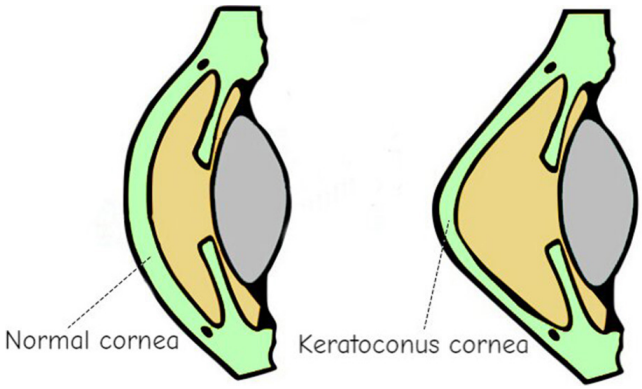

Fig. 1. Normal and keratoconus corneas

The prevalence of keratoconus is estimated between 50 and 230 for every 100000 people worldwide. Its prevalence is about 54.5 per 100000 people in the Caucasian population but increases to 229 per 100000 in Asians [4]. In Central India, this disease affects 1 person in 50 and approximately 1 person in 2000 in the United States [5]. In Morocco, no epidemiological study exists concerning the prevalence of keratoconus. The origin of this disease is multifactorial and the most significant risk factors for keratoconus are eye rubbing, allergy, asthma, eczema, and positive family history of keratoconus. Among these risk factors already cited, the most involved in keratoconus pathogenesis is eye rubbing [6].

Keratoconus detection and classification, according to its degree of severity, is a process that is generally based on the analysis of corneal topographic maps, its treatment also differs from optical correction to surgical interventions, depending on the degree of the disease [2]. keratoconus classification task is often carried out manually during consultations.

However, the big challenge is to discriminate the different stages of keratoconus, to be able to offer the right treatment for each case and stop the progression of the disease, especially in its forme fruste, which is difficult to detect because of the low expression of the disease relative to the indices of keratoconus presence. Thus, the daily clinical challenge is the cornea with borderline measurements. Specifically, the identification of the limit between the normal cornea and the forme fruste keratoconus. It is at this level that such a decision support system for the classification of keratoconus will be of great importance, to assist clinicians when classifying keratoconus.

The development of such decision support system, for keratoconus classification, can potentially improve healthcare, allowing specialists to make an objective and more robust decision and to obtain alternative treatment solutions before any surgery or heavy treatment that can alter physical condition.

The present paper proposes a keratoconus classification approach based on transfer learning method, a set of techniques which consist in transferring the knowledge acquired by CNN models, during the resolution of certain problems, to accomplish

new learning tasks which are not necessarily of the same context. In this sense, the six different classifiers VGG16, InceptionV3, MobileNet, DenseNet201, Xception and EfficientNetB0, pre-trained on specific datasets, are reused in this study for the classification of keratoconus by corneal topography analysis, taking advantages of the great capabilities of CNNs in classification problems [7].

2 Related works

A significant amount of research has been carried out in the context of the use of machine learning for keratoconus classification, according to its different stages, many of which were focused on the use of transfer learning techniques. Various pre-trained CNN models were used in these studies such as SqueezeNet (SqN), AlexNet (AlxN), ShuffleNet (SfN) and MobileNet-v2 (MbNV2), VGG16, VGG19, InceptionV3 (InCV3), ResNet152 (RsN152), InceptionResNetV2 (InCRsNV2), SVM. Table 1 below describes, in more detail, the research covered in the related works section, sorted by year of publication.

Table 1. Summary of related works sorted by year

Ref	Year	Models	Dataset	Classes	Accuracy
[8]	2022	PSO & VGG16	1500 images	3 classes	95.9%
[9]	2022	Two CNNs & VGG16	Over of 1900 patients	3 classes	Over 80%
[10]	2021	SqN, AlxN, SfN & MbNV2	444 cases	2 classes	98.3%
[11]	2021	VGG16 & a CNN	4000 images	2 classes	95.75%
[12]	2020	RsN152, VGG16 & InCV3	354 images	2 classes	95.8%, 93.1% & 93.1%
[13]	2020	InCV3	25 images (test set)	2 classes	73.33% for normal & 60% for keratoconus
[14]	2020	AlxN, VGG16 & VGG19	26736 images	4 classes	99.12%, 99.96% & 99.93%
[15]	2020	InCRsNV2	6465 images	5 classes	94.7%
[16]	2020	ResNet-based CNN	3000 images	3 classes	99.3%
[17]	2019	CNN	3000 images	2 classes	99.33%
[18]	2017	SVM	131 images	4 classes	92.6% to 98.0%

3 Methodology

3.1 Data collection

A total of 2924 topographic corneal images were captured, anonymously, using Pentacam device. Each corneal topographic image represents the cornea of a different patient. The retained part of these images is consisting of the four maps (corneal thickness, sagittal curvature, back and front elevations) in JPEG 1024x729 format as shown in the following Figure 2. Captured images have been classified and labeled manually, by specialists, considering three corneal classes, which are normal, suspicious and keratoconus corneal classes.

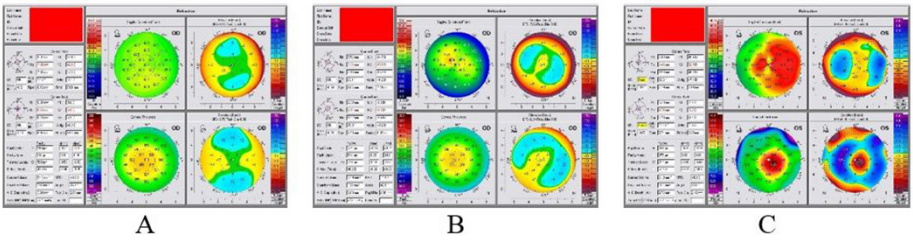

Fig. 2. Examples of corneal topographic images (A: normal cornea, B: suspicious cornea and C: keratoconus cornea)

All captured images contain annotations as well as color scales which can be harmful for the learning phase, a specific preprocessing of these images was necessary before they are used by different classifiers of the proposed system.

3.2 Images preprocessing

As shown in the Figure 2 above, each image is composed of Sagittal Curvature, Elevation Front, Corneal Thickness, and Elevation Back maps. Images also include color scale bars, metrics, texts, and numeric annotations that can represent noise and perturb the learning of different classifiers. In related works already cited, keratoconus classification was performed using corneal topographic images with all noise described above, in the most of studies. In the current study, a special preprocessing was applied to the original images to eliminate images noise.

The first step of image preprocessing consists of separating the four corneal maps in a JPEG format (265x265), while eliminating the color scale bars, metrics, textual and numerical annotations which risk reducing the performance of the final predictive system. The second step of image preprocessing consists of separating the corneal images composed of all the four maps in a JPEG format (605x665). The separation process of different corneal maps is carried out using the ImageJ tool [19] as illustrated in the Figure 3 below.

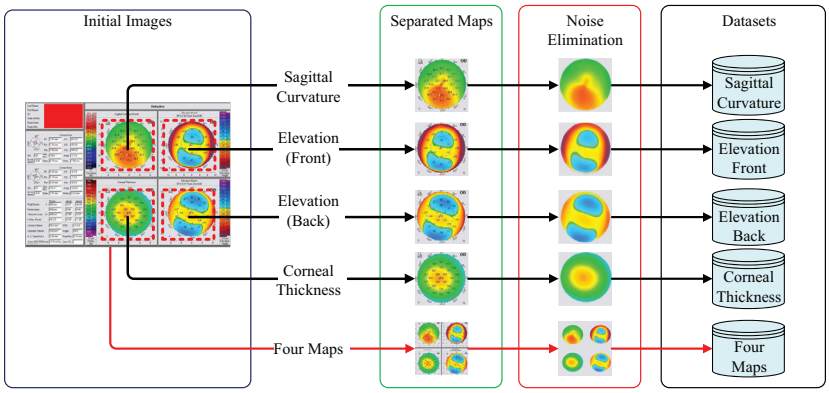

Fig. 3. Images separation process and datasets composition

Once the maps were separated, the next step is to remove the noise from images while preserving different colors. To do this, an elimination of dark outliers, followed by an elimination of bright outliers, with a radius of 15 and a threshold of 1 using ImajeJ tool, were applied to eliminate annotations, numerical and textual measurements that can affect the prediction accuracy of different models. Finally, five different datasets were composed of the noise-free images resulting from the already detailed preprocessing. The first dataset is composed of Sagittal Curvatures images, the second is made up of the Elevation Front images, the third is composed of the Corneal Thickness images, the fourth is represented by the Elevation Back images and the fifth is that made up of the four corneal maps.

3.3 Data augmentation

The original dataset used in this study is composed of a total of 2924 corneal topographic images. An ensemble of 341 Images were labeled as keratoconus (i.e. 12%), 1695 images were labeled as normal (i.e. 58%) and 888 images were labeled as suspicious (i.e. 30%). To balance the dataset, improve the performance of the proposed predictive system and ensure a better training of different classifiers, a data augmentation was applied to the different datasets [20]. In this study, the data augmentation is carried out by the application of some transformations using the Keras ImageDataGenerator class. Transformations include a random width and height shifts of the range of 0.1, horizontal flips of images, a random zoom of the images with a value of 0.2 and random rotation of training images by a value between 0 and 90 degrees.

It should be noted that the test data is not augmented and that the different models are tested on the real unmodified topographic images. The Figure 4 below indicates the images number before and after data augmentation.

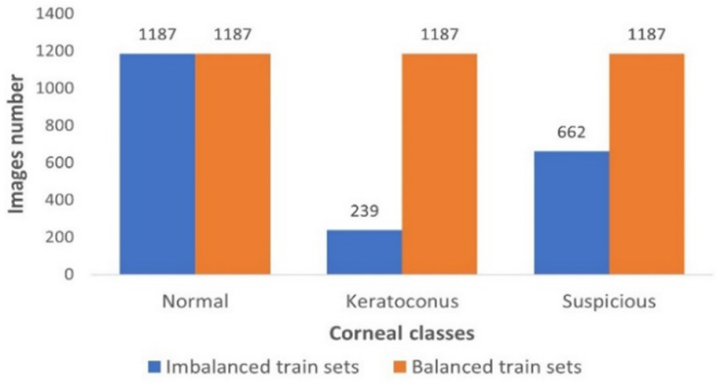

Fig. 4. Corneal classes distribution over different training datasets before and after data augmentation

3.4 Classification methodology

The proposed methodology of keratoconus classification in the current study, considering three classes of corneas, namely normal, suspicious and keratoconus, is described in Figure 5 bellow.

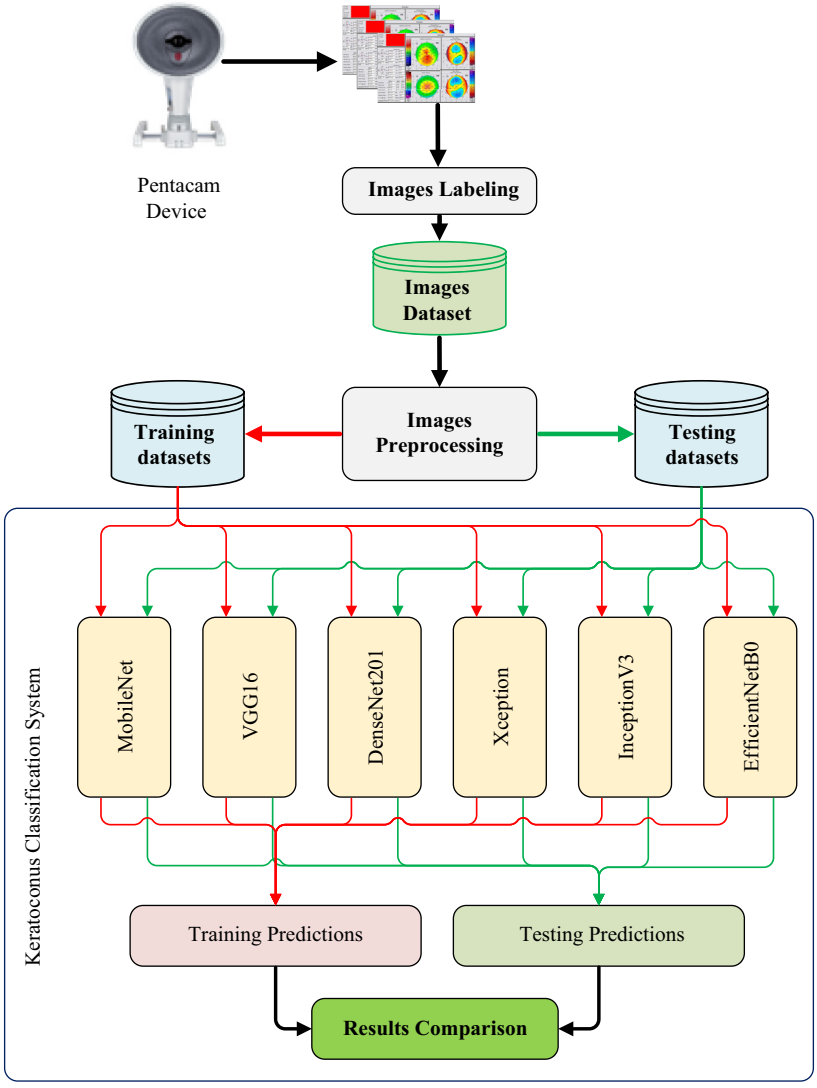

Fig. 5. Adopted methodology for keratoconus classification

In this study, corneal topographic images classification, of different datasets, is realized based on transfer learning technique. Six different pretrained CNN classifiers are used in the proposed method:

VGG-16. Characterized by its 16 trainable layers, this CNN classifier consists of 5 convolution blocks. The first 2 blocks are composed of 2 repeated 3x3 convolution layers with padding. The last 2 blocks have the same structure 3 repeated convolution layers instead of 2 layers. VGG16 also has a maximum pooling layer of 2x2 for down-sampling [21].

InceptionV3. As an extension of Google's GoogLeNet, InceptionV3 represents the 3rd version of a deep learning CNN architecture. Trained on the imageNet dataset, consisting of over a million images with 1000 different classes [22].

MobileNet. It is a type of CNN implemented especially for mobile vision systems and in-vehicle applications. The basic idea behind MobileNet is to use deep separable convolutions to compose simpler and lightweight deep neural networks that can have low latency for mobile and embedded devices [23]

DenseNet201. It is a type of CNN that uses dense connections between these different layers, through dense blocks, where all the layers are directly connected with each other. Each layer receives input from all previous layers and passes its own feature maps to all layers in the next level [24]. The version used in this study is DenseNet201.

Xception. Introduced by François Chollet [25], Extreme Inception is an architecture composed of 36 convolutional layers, which represent the feature extractor, these layers are structured in 14 modules with linear residual connections between them. Xception is a CNN with depth-separable convolution layers.

EfficientNetB0. The implementation of this CNN architecture is based on a study that demonstrated that scaling the depth, width and resolution of a Deep CNN, using a compound coefficient, can generate better performance. The version used in this study is the EfficientNetB0 [26].

Each model is trained separately on each of the different datasets, using the Adam optimizer with a learning rate of 0.001 over 30 epochs. The datasets were split into 70% for training and 30% for testing.

3.5 Evaluation metrics

To evaluate the prediction performance of the proposed classification system, the metrics used in this study are:

Execution time which represents the time taken by different models for the training and prediction phases.

Accuracy which is a simpler performance metric, this measure allows to calculate the percentage of good predictions compared to the set of predictions [27]. The accuracy is described by the following equation 1.

$$Accuracy = \frac{TP + TN}{TP + TN + FP + FN} \tag{1}$$

Precision that represents the number of observations correctly assigned to a given class relative to the total number, of correctly or incorrectly, classified positive samples [28]. Precision is represented by the following equation 2.

$$Precision = \frac{TP}{TP + FP} \tag{2}$$

Recall, this indicator, which is complementary to the metrics already mentioned, corresponds to the number of observations correctly attributed to a given class compared to the total number of positive samples [29]. The Recall is calculated using of the following equation 3.

$$Recall = \frac{TP}{TP + FN} \tag{3}$$

F1-score which is calculated by combining the Precision and the Recall, F1-score metric is generally preferred in the case of a classification with unbalanced classes. The F1-score is calculated as shown in the equation 4 below [30].

$$F1 - score = 2 * \frac{Precision * Recall}{Precision + Recall} \tag{4}$$

Where, True Positive (TP) represents the positive values that the system correctly predicts. For example, a keratoconus eye that the model predicts correctly. True Negative (TN) corresponds to negative values that are predicted correctly. This is the example of a normal eye that the model predicts as normal. False Positive (FP) represents the case of positive values that are predicted differently. This is the example of a normal eye which is predicted as keratoconus by the classifier. False Negative (FN) corresponds to actual values that are otherwise predicted. The case of a keratoconus eye that the model predicted as normal [27].

4 Results and discussion

4.1 Calculator and data descriptions

The simulation results are obtained using a calculator with an Intel(R) Core(TM) i5-6300U CPU @ 2.40GHz 2.40GHz processor, a RAM of 8.00 GB, Windows 8.1 Professional operating system, tensorflow and keras library in Python 3.7.4 on Jupyter notebooks. The distribution of corneal topographic images classes, in each of the five datasets used in this study, is described in table 2 below. Remind that to test the models on real images, validations are performed on real images of the original dataset, while trainings are performed on datasets after data augmentation.

Table 2. Datasets description

Classes	Total Images Number	Original Training Dataset	Augmented Training Dataset	Testing Dataset
Keratoconus	341	239	1187	102
Normal	1695	1187	1187	508
Suspicious	888	662	1187	266

4.2 Obtained results

Keratoconus classification in this study is carried out using VGG16, InceptionV3, MobileNet, DenseNet201, Xception and EfficientNetB0 CNN classifiers. Each of the

models used in this study is fine-tuned by freezing the pretrained weights of different layers, adding a fully connected layer followed by a softmax layer with 3 outputs and retraining the model using our five different datasets of 2924 corneal topographic images. As already mentioned, results are obtained using the Adam optimizer with a learning rate of 0.001 over 30 epochs and using uniform batches of six items. The datasets were split into 70% for training and 30% for testing. Table 3 below represents classification results obtained by the different CNN classifiers over different datasets.

Table 3. Obtained results using different classifiers

Dataset	Models	Accuracy	Precision	Recall	F1-Score	Execution Time
Corneal Thickness	VGG16	97.60%	95%	96%	96%	2h17min7s
	InceptionV3	88.92%	87%	83%	85%	29min28s
	MobileNet	97.49%	97%	95%	96%	17min20s
	DenseNet201	97.60%	96%	96%	96%	1h58min2s
	Xception	95.20%	93%	92%	93%	1h5min25s
	EfficientNetB0	57.99%	19%	33%	24%	37min34s
Elevation Back	VGG16	93.72%	92%	93%	92%	2h12min9s
	InceptionV3	84.36%	83%	84%	83%	27min19s
	MobileNet	93.94%	92%	92%	92%	16min49s
	DenseNet201	94.86%	92%	92%	92%	1h42min37s
	Xception	89.61%	88%	88%	88%	1h2min30s
	EfficientNetB0	30.36%	10%	33%	16%	33min9s
Elevation Front	VGG16	90.75%	91%	88%	89%	2h11min22s
	InceptionV3	78.53%	79%	76%	77%	27min23s
	MobileNet	95.31%	95%	93%	94%	16min40s
	DenseNet201	96.23%	94%	94%	94%	1h43min42s
	Xception	83.90%	82%	80%	81%	1h4min23s
	EfficientNetB0	30.36%	10%	33%	16%	33min14s
Sagittal Curvature	VGG16	96.00%	95%	93%	94%	2h10min25s
	InceptionV3	78.76%	79%	77%	78%	26min58s
	MobileNet	95.20%	95%	92%	94%	16min26s
	DenseNet201	93.83%	93%	92%	92%	1h43min55s
	Xception	81.96%	82%	82%	82%	1h3min25s
	EfficientNetB0	57.99%	19%	33%	24%	32min55s
Four maps	VGG16	98.51%	97%	98%	98%	2h11min20s
	InceptionV3	91.78%	90%	90%	90%	27min14s
	MobileNet	98.74%	98%	98%	98%	16min47s
	DenseNet201	99.31%	99%	98%	99%	1h45min18s
	Xception	91.43%	89%	91%	90%	1h9min31s
	EfficientNetB0	30.36%	10%	33%	16%	42min25s

The Figure 6 below illustrates DenseNet201 classifier accuracy curves on the corneal thickness, elevation back, elevation front, sagittal curvature and the four corneal maps datasets respectively.

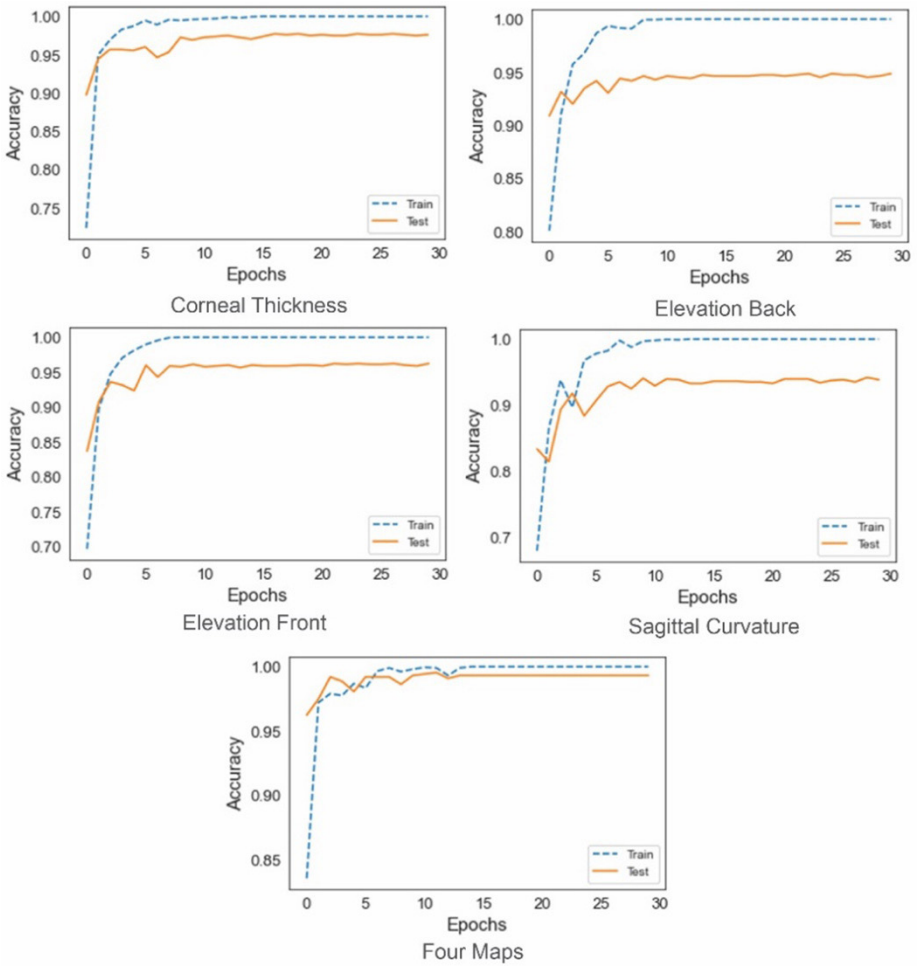

Fig. 6. DenseNet201 classifier accuracy curves over different datasets

Figure 7 below shows DenseNet201 classifier loss curves on the corneal thickness, elevation back, elevation front, sagittal curvature and the four corneal maps datasets respectively.

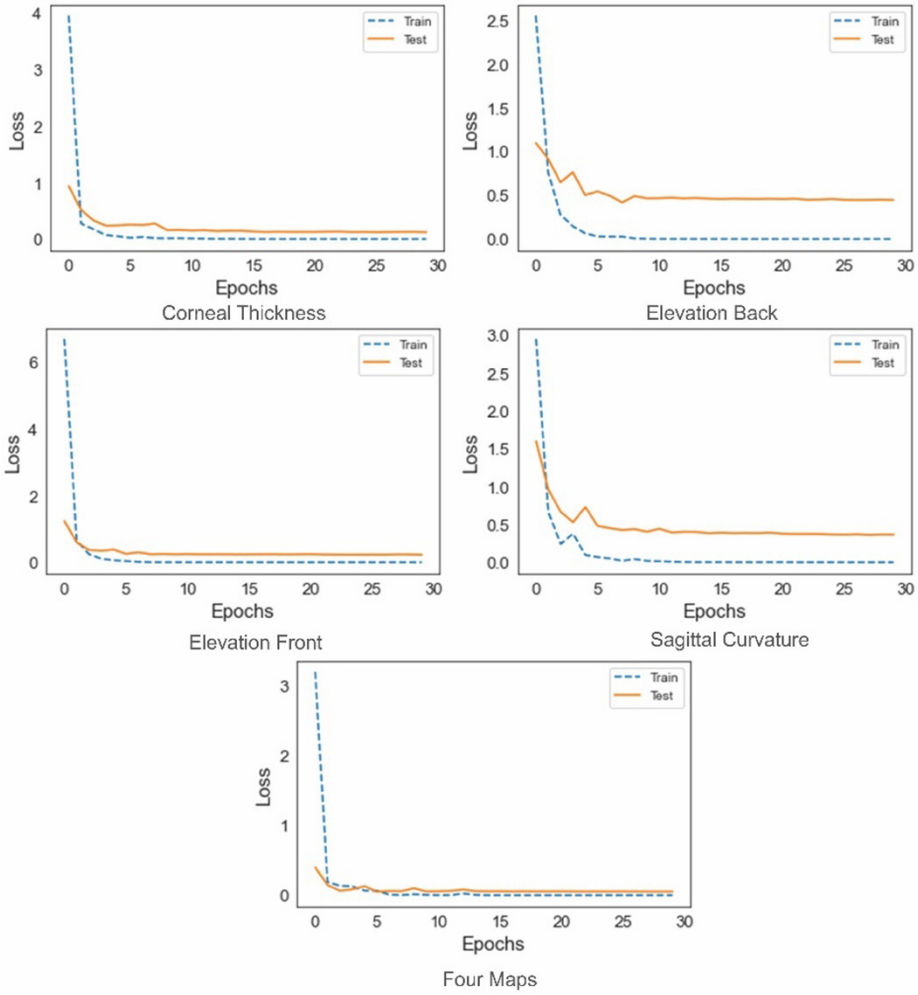

Fig. 7. DenseNet201 classifier loss curves over different datasets

The Figure 8 below represents the confusion matrixes for the DenseNet201 classifier over different datasets used in this study.

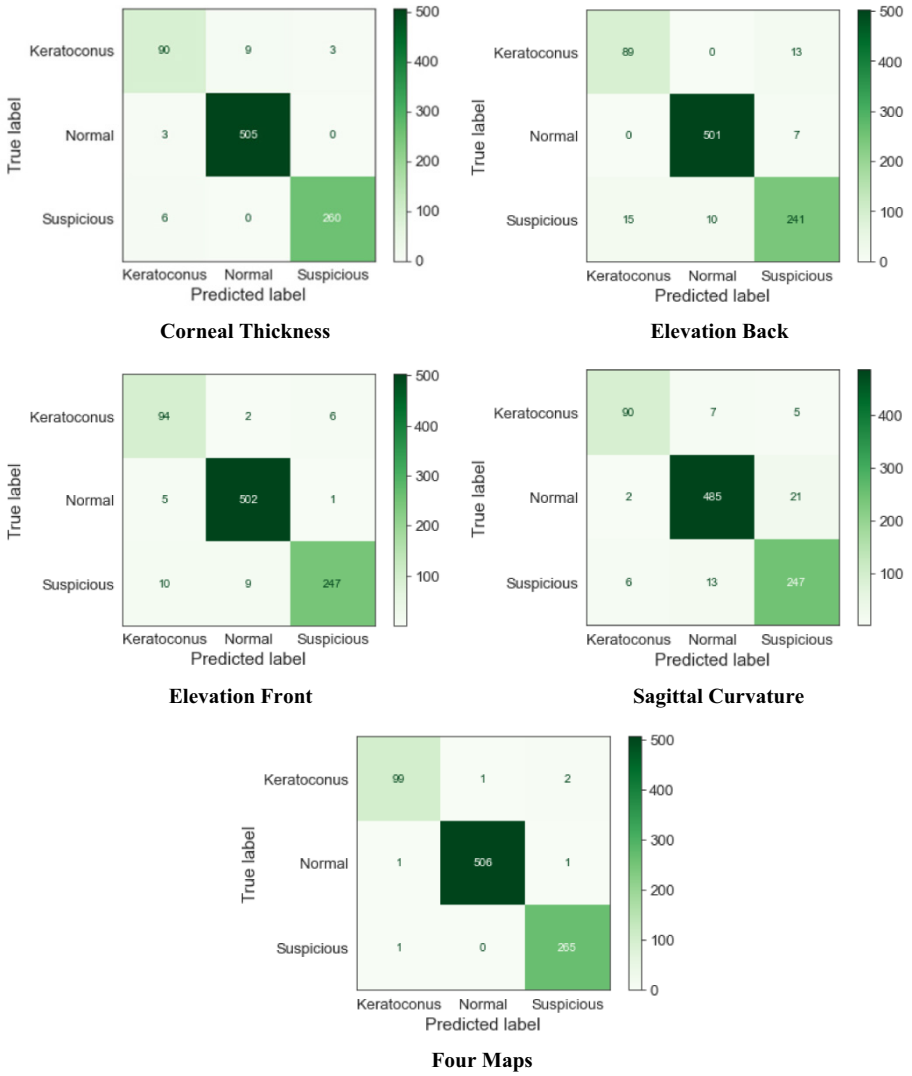

Fig. 8. DenseNet201 classifier confusion matrixes over different datasets

4.3 Discussion

Figures 6, 7 and 8 above indicate that DenseNet201 model can discriminate between normal, suspicious and keratoconus corneas with an accuracy which exceed 90%.

Table 3 above represents the performance of the different classifiers, trained individually, on the five different datasets. On the corneal thickness dataset, VGG16 and DenseNet201 allow keratoconus classification with an accuracy of 97.60%, representing the best classifiers on this dataset, considering classification accuracy. Considering the execution time, VGG16 and DenseNet201 take 2h17min7s and 1h58min2s

respectively to classify different images on the corneal thickness dataset. On the same dataset, the MobileNet allows classification with an accuracy of around 97.49% with an execution time of 17min20s, representing the fastest classifier on this dataset. The performance of MobileNet is also better, especially considering the accuracy/execution time rate. Using the Elevation back dataset, DenseNet201 represents the best model, with an accuracy of 94.86%, followed by VGG16 and MobileNet with a classification accuracy of around 93.72% and 93.94% respectively. In terms of execution time, MobileNet is the fastest classifier, allowing classification in about 16min49s. DenseNet201 and VGG16 classifiers take 1h42min37s and 2h12min9s respectively to classify different images.

On the Front Elevation dataset, DenseNet201 achieves an accuracy of 96.23% in 1h43min42s. The second classifier is MobileNet, this model reaches an accuracy of 95.31%, in about 16min40s, marking the execution time the most restricted over this dataset.

In the case of Sagittal Curvature dataset, the VGG16 represents the best model with an accuracy of 96.00%, while consuming 2h10min25s. The second classifier on this dataset is the MobileNet with an accuracy of 95.20% in 16min26s run time.

On the last dataset, composed of the four corneal maps, the best classification performance is achieved by the DenseNet201 model, which reaches a classification accuracy of 99.31% with an execution time of 1h45min18s, followed by MobileNet and VGG16 which achieve classification accuracy of 98.74% and 98.51% respectively. MobileNet and VGG16 take 16min47s and 2h11min20s respectively.

Generally, the best performing classifier on most datasets, considering classification accuracy, is DenseNet201. But considering the execution time, MobileNet is the fastest, with an execution time that does not exceed 18 minutes. VGG16 is retained as the slowest classifier with an execution time varying between 2h10min and 2h17min over all datasets. The lowest performance, over all datasets, are those achieved EfficientNetB0 classifier. EfficientNetB0 is marked as the least efficient model, with a classification accuracy of 57.99%, 30.36%, 30.36%, 57.99% and 30.36% on the dataset composed of corneal thickness, elevation back, elevation front, sagittal curvature and four maps respectively.

5 Conclusion

This paper proposed a transfer learning-based system, using pretrained CNN classifiers, for keratoconus classification from corneal topographic images. In this context, five different datasets were built, composed of corneal thickness, elevation back, elevation front, sagittal curvature and four corneal maps respectively, to ensure a better learning for the different deep learning-based classifiers. Obtained results indicated that transfer learning can improve systems to accurately classify keratoconus in its different stages. Such systems could potentially assist specialists in the keratoconus classification task, which is still made manually.

6 Acknowledgment

We would like to express our gratitude to the Professor Hazem Abdelmotaal, Department of Ophthalmology, Faculty of Medicine, University of Assiut, for his generosity and his spirit of scientific sharing, which contributed to the good conduct of this work.

7 References

[1] Asroui L, Mehanna C-J, Salloum A, et al. (2021). Repeatability of Zone Averages Compared to Single-Point Measurements of Maximal Curvature in Keratoconus. Am J Ophthalmol, 221:226–234. https://doi.org/10.1016/j.ajo.2020.08.011

[2] Lupasco T. (2019). Thesis: Etude comparative du programme de différenciation terminale de l'épithélium de la cornée normale et des patients atteints de kératocône. Organs of the senses. Paul Sabatier University – Toulouse III.

[3] Tabibian D, Hafezi F. (2014). Maladies de l'oeil et trisomie 21: une mise à jour. Revue suisse de pédagogie spécialisée, 1:34. https://doi.org/10.1016/S1773-035X(14)72440-2

[4] Rupin A. (2015). Thesis: Efficacité à 1 an du protocole accéléré de cross-linking versus crosslinking conventionnel dans le traitement du kératocône évolutif: à propos de 64 cas traités au CHRU de Lille. Exercise Thesis, University of Law and Health, Lille; 1969–2017, France.

[5] Lin S. R, Ladas J. G, Bahadur G. G, et al. (2019). A Review of Machine Learning Techniques for Keratoconus Detection and Refractive Surgery Screening. Semin Ophthalmol, 34:317–326. https://doi.org/10.1080/08820538.2019.1620812

[6] Hashemi H, Heydarian S, Hooshmand E, et al. (2020). The Prevalence and Risk Factors for Keratoconus: A Systematic Review and Meta-Analysis. Cornea, 39:263–270. https://doi.org/10.1097/ICO.0000000000002150

[7] Gu Y, Zalkikar A, Liu M, et al. (2021). Predicting Medication Adherence Using Ensemble Learning and Deep Learning Models with Large Scale Healthcare Data. Sci Rep, 11. https://doi.org/10.1038/s41598-021-98387-w

[8] Subramanian P, Ramesh G. P. (2022). Keratoconus Classification with Convolutional Neural Networks Using Segmentation and Index Quantification of Eye Topography Images by Particle Swarm Optimisation. Biomed Res Int, 2022. https://doi.org/10.1155/2022/8119685

[9] Schatteburg J, Langenbucher A. (2022). Protocol for the Diagnosis of Keratoconus Using Convolutional Neural Networks. PLoS One, 17. https://doi.org/10.1371/journal.pone.0264219

[10] Al-Timemy A. H, Ghaeb N. H, Mosa Z. M, et al. (2021). Deep Transfer Learning for Improved Detection of Keratoconus Using Corneal Topographic Maps. Cognit Comput. https://doi.org/10.1007/s12559-021-09880-3

[11] Kuo B. I, Chang W. Y, Liao T. S, et al. (2010). Keratoconus Screening Based on Deep Learning Approach of Corneal Topography. Transl Vis Sci Technol, 9:53. https://doi.org/10.1167/tvst.9.2.53

[12] Zaki W. M. D. W, Daud M. M, Saad A. H, et al. (2021). A Mobile Solution for Lateral Segment Photographed Images Based Deep Keratoconus Screening Method. International Journal of Integrated Engineering, 13.

[13] Sonar H, Kadam A, Bhoir P, et al. (2020). Detection of Keratoconus Disease. ITM Web of Conferences, 32. https://doi.org/10.1051/itmconf/20203203019

[14] Elsawy A, Abdel-Mottaleb M, Shousha M. A, et al. (2020). Diagnosis of Corneal Pathologies Using Deep Learning. Ophthalmic Technologies XXX, 11218:150–160. https://doi.org/10.1117/12.2552478

[15] Xie Y, Zhao L, Yang X, et al. (2020). Screening Candidates for Refractive Surgery with Corneal Tomographic–Based Deep Learning. JAMA Ophthalmol, 138:519–526. https://doi.org/10.1001/jamaophthalmol.2020.0507
[16] Zéboulon P, Debellemanière G, Bouvet M, et al. (2020). Corneal Topography Raw Data Classification Using a Convolutional Neural Network. Am J Ophthalmol, 219:33–39. https://doi.org/10.1016/j.ajo.2020.06.005
[17] Lavric A, Valentin P. (2019). KeratoDetect: Keratoconus Detection Algorithm Using Convolutional Neural Networks. Comput Intell Neurosci, 2019. https://doi.org/10.1155/2019/8162567
[18] Hidalgo I. R, Rozema J. J, Saad A, et al. (2017). Validation of an Objective Keratoconus Detection System Implemented in a Scheimpflug Tomographer and Comparison with Other Methods. Cornea, 36:689–695. https://doi.org/10.1097/ICO.0000000000001194
[19] RSB Home Page. https://imagej.nih.gov/. Accessed: February 2022.
[20] Shorten C, Khoshgoftaar T. M. (2019). A survey on Image Data Augmentation for Deep Learning. J Big Data, 6. https://doi.org/10.1186/s40537-019-0197-0
[21] Elnakib A, Amer H. M, Abou-Chadi F. E. Z. et al. (2020). Early Lung Cancer Detection Using Deep Learning Optimization. International Journal of Online and Biomedical Engineering (iJOE), 16:82–94. https://doi.org/10.3991/ijoe.v16i06.13657
[22] Nguyen L, Lin D, Lin Z, et al. (2018). Deep CNNs for Microscopic Image Classification by Exploiting Transfer Learning and Feature Concatenation. IEEE Int Symp Circuits Syst Proc. https://doi.org/10.1109/ISCAS.2018.8351550
[23] Safuan S. N. M, Tomari M. R. M, Zakaria W. N. W, et al. (2022). Cross Validation Analysis of Convolutional Neural Network Variants with Various White Blood Cells Datasets for the Classification Task. International Journal of Online and Biomedical Engineering (iJOE), 18:123–140. https://doi.org/10.3991/ijoe.v18i02.27321
[24] Huang G, Liu Z, van der Maaten L, et al. (2018). Densely Connected Convolutional Networks. ArXiv. Available at: http://arxiv.org/abs/1608.06993. Accessed: January 2022.
[25] Chollet F. (2017). Xception: Deep Learning with Depthwise Separable Convolutions. Proc IEEE Comput Soc Conf Comput Vis Pattern Recognit, 1800–1807. https://doi.org/10.1109/CVPR.2017.195
[26] Tan M, Le Q V. (2020). EfficientNet: Rethinking Model Scaling for Convolutional Neural Networks. ArXiv. Available at: http://arxiv.org/abs/1905.11946. Accessed: March 2022.
[27] Mahmoud H. A. H, Mengash H. A. (2021). Automated Keratoconus Detection by 3D Corneal Images Reconstruction. Sensors, 21. https://doi.org/10.3390/s21072326
[28] Tatbul, N, Tae J. L, Stan Z, et al. (2018). Precision and Recall for Time Series. Advances in neural information processing systems, 31.
[29] Amiri E, Roozbakhsh Z, Amiri S, Asadi M. H, et al. (2020). Detection of Topographic Images of Keratoconus Disease Using Machine Vision. International Journal of Engineering Science and Application, 4:145–150.
[30] Aatila M, Lachgar M, Hrimech H, Kartit A, et al. (2021). Keratoconus Severity Classification Using Features Selection and Machine Learning Algorithms. Comput Math Methods Med, 2021. https://doi.org/10.1155/2021/9979560

8 Authors

Mustapha Aatila is a Ph.D. Student at the LTI Laboratory, ENSA, Chouaib Doukkali University, El Jadida, Morocco. He received the M.S degree in software quality from Cadi Ayyad University, Morocco in 2009. His research focuses on artificial

intelligence, machine learning and deep learning applied to the ophthalmology field, particularly in keratoconus detection and classification.

Mohamed Lachgar is a professor in Computer Science at the National School of Applied Sciences, Chouaib Doukkali University, El Jadida, Morocco. He received his Ph.D. in Computer Science at the Cadi Ayyad University in 2017. His research interests are in the areas of automation tools development in embedded software, software modeling & design, metamodel design, model transformation, model verification & validation method, machine learning and deep learning.

Hamid Hrimech is an associate professor at University Hassan 1st at Morocco's ENSA department of computer science and mathematics. In 2009, he received a Ph.D. in Computer Science from Arts et Métiers ParisTech in France. Artificial intelligence, collaborative interactions in a collaborative virtual environment, and driving simulation are among his research interests.

Ali Kartit is an associate Professor at the National Schools of Applied Sciences (ENSA) University Chouaib Doukkali of El Jadida, Morocco. His Ph.D. in Computer Science from the Faculty of Sciences, University MohamedVI of Rabat, in 2011. His research interests are information systems security, network security, cloud security, research in encrypted data, IDS/IPS, Firewall and artificial intelligence applied to security.

Article submitted 2022-06-29. Resubmitted 2022-08-15. Final acceptance 2022-08-23. Final version published as submitted by the authors.